



Energy Demand of a Single-train Movement in Viaduct Structure Using Multi Conductor Earthing Systems

T. Chuchit, C. Sumpavakup, and T. Kulworawanichpong*

Abstract— This paper presents energy demand at a traction substation for a single-train movement. To be more realistic and complete, the rail potential should be calculated while the train is moving, which plays an important role in the design of electrified railway service. A single-train simulator model was developed to collect and evaluate stray currents in the viaduct structure using an earthing model, which consists of NGM, DGM, and N-DGM, with multi-conductor systems and the calculation of power flow, was used in the study using the current injections methods (CIM). In addition, this model also calculates the voltage in the metal structure. The algorithm of the train movement is used in conjunction with the calculation of the power flow using the MATLAB/M-file and applied to the MRT Purple Line in Bangkok, Thailand as a case study. It is expected to show the efficiency of the single-train moment modelling to calculate the rail potential, the structure voltage, energy demand at the substation, power loss and, voltage profile of the train during the movement of the train. In addition, by comparing the earthing model by NGM, DGM and N-DGM methods, the DGM and N-DGM models have similar energy demand and are less than 0.087% of the NGM model.

Keywords— Energy demand, single-train movement, viaduct structure, multi-conductor earthing systems.

1. INTRODUCTION

DC railway system is widely used in metropolitan areas around the world. It was developed to facilitate mass transit system and reduce traffic. Electric power is supplied to a train using a third rail, and running rails are used as a return conductor for traction current. Due to insufficient insulation between the running rails and the earth, some electric currents may flow through the earth back to the traction substation. These currents are known as leakage or stray currents. This situation causes electrical corrosion and damage to nearby structures and infrastructures [1-4]. Generally, direct measurement of stray currents is difficult; hence, measuring voltage between the running rail and earth is done instead. The voltage difference is called rail potential. In addition to stray current problems, rail potential may jeopardize person's safety with a permissible touch voltage not over than 120 V of a period which more than 300 secs for DC railway systems with EN 50122-1 standard [5]. However, the rail potential should not exceed +5 V within 24-hour with EN 50122-2 standard [6-7]. To avoid or reduce these defects, the rail potential must be evaluated and controlled. Therefore, it is necessary to model for considering the rail potential and preliminary study and evaluation.

In recent years, some research has been carried out on

the simulations of train movements with different models and methods of observing rail potential and stray currents [8-10]. Most research calculates the rail potential instead of calculating the stray current directly [11], which is a popular method used to evaluate the stray current of the DC train system. Calculating the stray current in a tunnel structure with a two-sided power station [12], using a transmission line model technique. Calculating the flow of current and voltage in the tunnel structure including electricity and electric potential at rails using distributed and group parameters [13], where the use of distributed parameters (DP) is calculated using the transmission line model technique and the Lump parameters (LP) is calculated using STM (sparse tableau method), both models are based on two-sided power distribution systems that are considered underground metal pipes. After that, the model was developed using the MATLAB GUI by LP calculation method [14] using the STM technique as well as the previous article. The simulation of stray current using CDEGS (current distribution, electromagnetic fields, soil structure analysis), by CDEGS program compared to programs MATLAB/Simulink programs for the case of differences in soil layers [15] which is considered the stray current when the soil electrical conductivity changes in each solid layer. And research that calculates the current and voltage at the rails, including the analysis of the rail voltage along the length of the rails and the remote impact in normal working conditions and short circuit with a single power supply system and the model also considered the rail length on the side of the power station [16] using the transmission line model technique. In addition, it simulates the movement of a single train that has considered the electric potential at the rail [17].

A study of the train movement model developed a model of a single-train by pivoting a metal structure under tracks. This article focuses on the construction of a single-train movement model, considering the rail

T. Chuchit is with the School of Electrical Engineering, Suranaree University of Technology, Nakhon Ratchasima 30000, Thailand.

C. Sumpavakup is with the College of Industrial Technology, King Mongkut's University of Technology North Bangkok, Bangkok 10800, Thailand.

T. Kulworawanichpong is with the School of Electrical Engineering, Suranaree University of Technology, Nakhon Ratchasima 30000, Thailand.

*Corresponding author: T. Kulworawanichpong; Phone: +66-8-8583-7207; E-mail: thanatchai@gmail.com.

potential and voltage in structures using multi-conductor systems. A power flow calculation is applied in the study using the current injection methods (CIM) [17, 18], which it was widely adopted as a technique for power network solution in the DC railway power supply study to calculate the rail potential, structure voltage, energy demand at substations and, voltage profile of the train during the train movement.

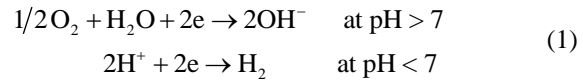
Train movement and power flow algorithms are implemented using MATLAB/M-file. A single-train movement simulation is done in normal condition, using the MRT Purple Line in Bangkok, Thailand, as a case study.

2. STRAY CURRENT

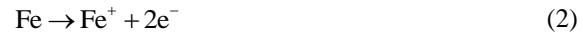
While the train moves along the running rail with the worst insulation between the running rail and sleeper causing the stray current occurs. Thus, this paper focuses on the corrosion stray current of the metal structure. The rails are installed on sleepers, which in turn are placed on the ballast, sub-ballast, sometimes an insulating layer, and earth. A concrete slab permanent way is an alternative to sleepers and ballast. High track-to-earth resistance is found in cases where a new track is laid with well-insulating ballast on exceedingly dry sandy soils or where the rails are specifically insulated for the sleepers. In most cases, however, the track-to-earth resistance is so low that a part of the return current will flow through the earth, whereby the soil acts as an electrolyte. Currents leaving the running rails can cause stray current corrosion on metal pipes and other underground metallic installations in the vicinity of DC traction railway [1-10].

The electric current passes from the running rail to the earth will cause corrosion of the electrochemical process, in this case, raises two parallel processes. For two parallel processes divided the corrosion due to stray current occurs at the anode where current leaves metal into the electrolyte, such as clay or steel reinforced concrete structure, will cause an anodic reaction. In addition, the cathode where current leaves electrolyte into metal will cause a cathodic reaction, both of two processes will occur simultaneously, the cathode reaction

on the leakage current into the metal structure as part of the reaction corrosion occurs, using iron as an example [1] as follows:



where, pH is the pH of the reaction anodic reaction while the leakage current is flowing out of the metal structure to the electrolyte reactions, corrosion anode result. By anodic reaction or oxidation (dissolution) of metal [1] equation is:



The assessment of stray currents in DC rail transit systems is done to prevent damage to the structure and nearby structures. The important factor that influences stray current is the conductance per unit length between track and earth. The rate of corrosion is the main parameter used in risk assessment. Experience suggests that there is will be no damage in the tracks over a period of 25 years if the average stray current per unit length does not exceed 2.5 mA/m[2]. As it is impractical to measure the stray currents directly, the conductance and potential of the running rails against earth are assessed in accordance with EN 50122-2 standard [5].

3. TRAIN MOVEMENT CALCULATION

The speed, acceleration, and position are the important factors and necessitated to be taken into consideration. The train has to travel with the speed complied with limited conditions such as the terrain and curvature. Additionally, the electric power required by the train is necessary to be known for power flow calculation in the simulation. Train movement was shown in equation (3) namely, the forces related are the tractive force, the gravitational force/gradient force and the resistance forces. Fig. 1 demonstrates the free body diagram of the train moving upwards on the slope including the mentioned forces exerting on it [17, 18].

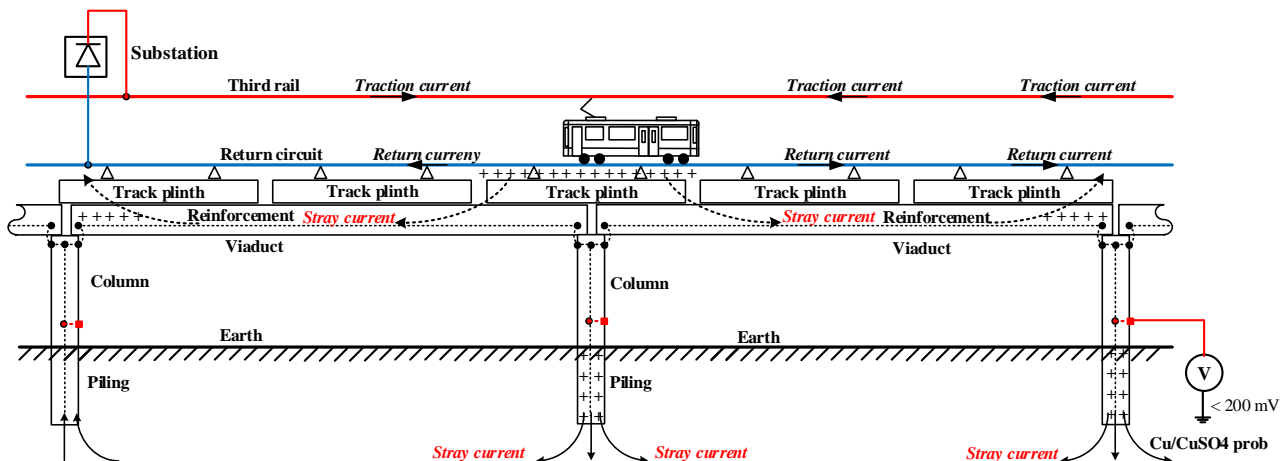


Fig. 1. Stray current path of a viaduct structure.

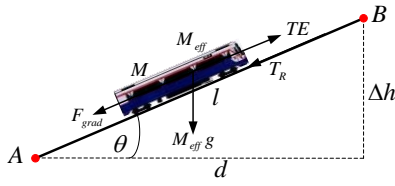


Fig. 2. Free body diagram of the train.

$$F = TE - F_{grad} - T_R = M_{eff} \alpha \quad (3)$$

where M_{eff} is the effective mass (kg),
 TE is the tractive force (N),
 T_R is train resistance (N),
 F_{grad} is gradient force (N),
 α is train acceleration (m/s²),
 F is the total force (N).

Gradient force

Gradient force is a range of slope or range of horizontal plane from point A to point B, as shown in Fig. 2. Gradient force or force due to the slope of motion [18] is obtained as in (4):

$$F_{grad} = M_{eff} g \sin \theta = \frac{M_{eff} g \Delta h}{l} \quad (4)$$

where g is the acceleration due to gravity, 9.8 m/s²,
 Δh is a rise of the slope,
 l is the slope length,
 θ is the slope's angle with respect to the horizontal line.

Train resistance

The train resistance formula for a train set is defined based on JIS E 6002, Japanese national Industrial Standard (JIS) [19] as shown in (5)

$$T_R = (1.65 + 0.0247v)W_m + (0.78 + 0.0028v)W_t + \{0.78 + 0.0078(n-1)\}v^2 \quad (5)$$

where T_R is train resistance (kgf)
 v is train Speed (km/h)
 W_m is the weight of all motor cars in a train (ton)
 W_t is the weight of all trailer cars in a train (ton)
 n is the Number of cars in a train

Electric power of the train

The power consumed by a train corresponding to the tractive effort (TE) and instantaneous speed v is given

by the following equation [20]:

$$P = \frac{TE \times v}{\eta} \quad (6)$$

where η denotes the efficiency of the power conversion in terms of electrical input power to the mechanical output power at the wheels.

Train motion

Train motion between two stations is typically characterized by the trajectory of the train's time-speed curve. Basic operation of train movement is generally characterised under 4 operating modes which are accelerating mode, cruising or constant-speed mode, coasting mode, and braking mode, as shown in Fig. 3. [17, 21]

In this article, train motion modelling is based on proportional control principle [22], following a pre-defined speed profile. The proportional control is shown in Fig. 4. The train modelling is divided into three modes: running mode, braking mode and stop mode.

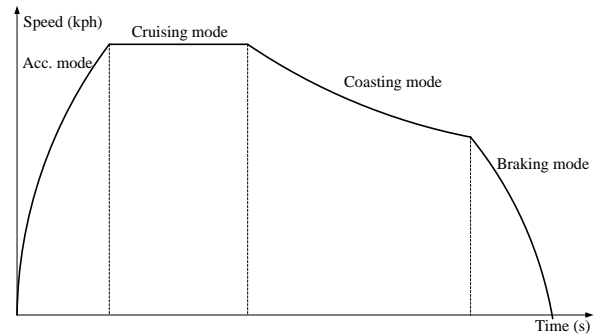


Fig. 3 Train's speed profile.

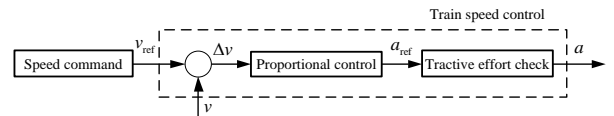


Fig. 4 proportional control.

Train speed and position update

Train speed and position are updated using (7) and (8), respectively, where v_{i+1} and v_i are train speeds after and before update, Δt is the time step, s_{i+1} and s_i are train positions after and before update and, a is a train acceleration.

$$v_{i+1} = v_i + a\Delta t \quad (7)$$

$$s_{i+1} = s_i + v_i\Delta t + \frac{1}{2}a\Delta t^2 \quad (8)$$

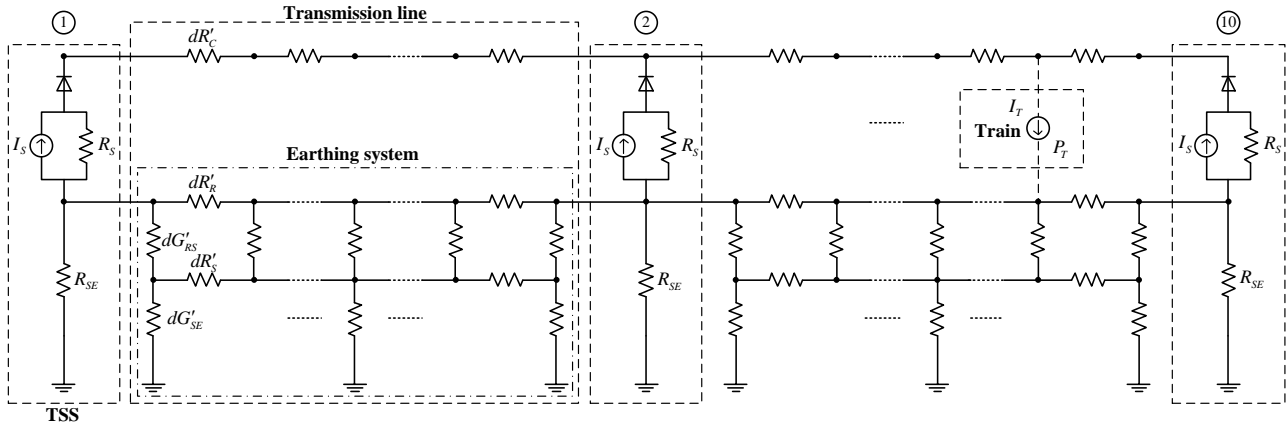


Fig. 5. The proposed DC railway single-train system model for non-distributed grounding models.

4. SINGLE-TRAIN SIMULATION

Single-train model

- Traction substation model

The traction substation receives electricity from the AC power network and it's rectified to be a DC system to supply the DC railway system. In this paper, the traction substation is considered as the Norton equivalent circuit, a current source (I_s) in parallel with the substation resistance (R_s), connected to the suitable diode and the earthing resistance (R_{SE}), as shown in Fig. 5. as a traction substation (TSS) block, where C refers to the conductor rail/third rail, R refers to the running rails. In the simulation, the earthing resistance is given to be infinite since the traction substation is not directly grounded or floated through the protective devices [17, 21].

- Transmission line model

The transmission line is considered to be a distance-based distribution model, separated by distance d , as shown in Fig. 5. as the transmission line block between bus p and q . The conductor rail is represented by third rail's resistor (R'_C). In the same manner, the running rail is represented by running rail's resistor (R'_R) and the rail-to-structure resistance along the tracks is represented by the rail-to-structure conductance per unit length (G'_{RS}). The metal structure under the rails along the tracks is represented by structure's resistor (R'_S) and the structure-to-earth resistance along the tracks is represented by the structure-to-earth conductance per unit length (G'_{SE}). Therefore, the rail potential is the voltage distributed across the rails, and this article also introduces the voltage in the structure.

This research considers the earthing models of the transmission line as three models, showing the following details.

1. Normally grounding models (NGM)

NGM is a model based on EN 50122-2 standard that is generally used for determining the rail potential without considering the viaduct structure, which is illustrated as

in Fig. 6. and to make it easier to simulate results as shown in Fig. 7. which consists of running rail's resistor and rail-to-earth conductance per unit length (G'_{RE}).

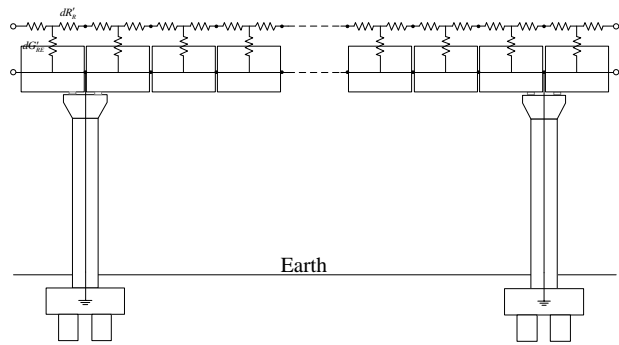


Fig. 6 NGM.

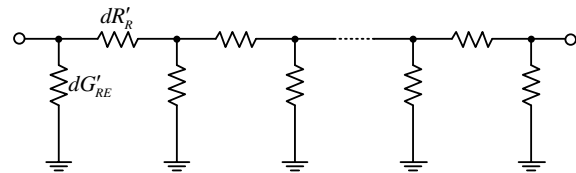


Fig. 7. Simple model of NGM.

2. Distributed grounding models (DGM)

DGM is a model for determining the rail potentials and structure voltage by considering the viaduct structure, which is illustrated in Fig. 8., And to make it easier to simulate, can be written as shown in Fig. 9., which consists of running rail's resistor, rail-to-earth conductance, structure's resistor and structure-to-earth conductance per unit length.

3. Non-distributed grounding models (N-DGM)

DGM is a model for determining the rail potentials and structure voltage are by considering the viaduct structure, which is illustrated in Fig. 8., And to make it easier to simulate, can be written as shown in Fig. 9. The model is the same as the DGM, but only with the grounding at piers of the structure.

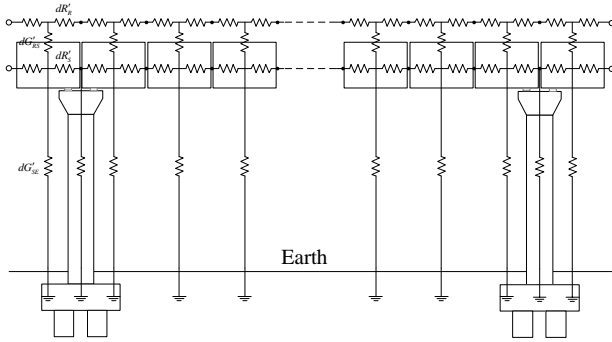


Fig. 8 DGM.

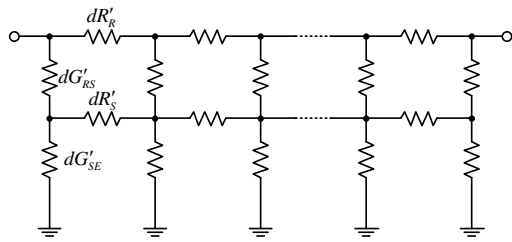


Fig. 9 Simple model of DGM.

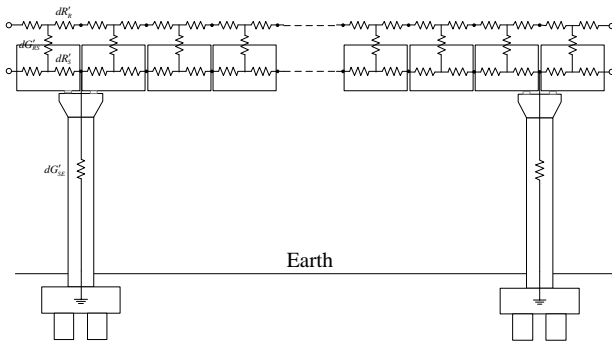


Fig. 10. N-DGM.

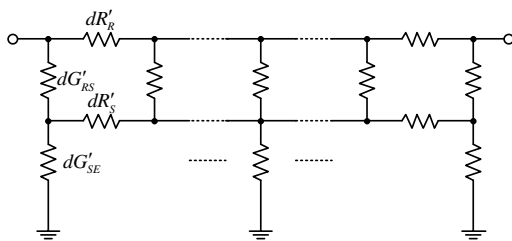


Fig. 11. Simple model of N-DGM.

- Train model

The CIM has been used in the power flow calculation. The train should be modelled as the current source (I_T) between the conductor rail (third rail) and running rail.

Power flow calculation

To obtain traction substations' voltages, train voltage, consumed power for each substation, rail potential, and power losses in the system, a power flow of the train network are done. In this paper, the current injections method is applied in the power flow calculation with the multi-conductor system due to having three conductors per bus. Power network is based on nodal analysis

including rectifier substations and single-train using the proposed model, illustrated in Fig. 5. The solution can be obtained by solving the nodal equations in (9) and giving all bus voltages are initially zero [17, 21].

$$[I] = [G][V] \quad (9)$$

The conductance matrices $[G]$ are formed by the conductance submatrices for each bus. Therefore, the ability to create $[G]$ depends on the multi-conductor system connected to each bus from the grounding model that has been proposed. It can divide multiple conductors into two types: two-level and three-level conductor systems as shown below.

1. Two-level conductor systems

A two-level conductor system per bus is a system that is used with a NGM based on EN 50122-2 standards. The conductance matrices $[G]$ are formed by the conductance submatrices for each bus as shown in (10)-(12) [17], where $[G_s]$ denotes the substation conductance submatrix considered only the substation buses, $[G_{pq}]$ denotes the transmission conductance submatrix between bus p and q including the conductor rail conductance and the running rail conductance, and $[G_{pp}]$, $[G_{qq}]$ denote the rail-to-earth conductance matrix.

$$[G_s] = \begin{bmatrix} \frac{1}{R_s} & -\frac{1}{R_s} \\ -\frac{1}{R_s} & \frac{1}{R_s} + \frac{1}{R_{se}} \end{bmatrix} \quad (10)$$

$$[G_{pq}] = [G_{qp}] = \begin{bmatrix} \frac{1}{dR'_c} & 0 \\ 0 & \frac{1}{dR'_r} \end{bmatrix} \quad (11)$$

$$[G_{pp}]_{RE} = [G_{qq}]_{RE} = \begin{bmatrix} 0 & 0 \\ 0 & dG'_{re} \end{bmatrix} \quad (12)$$

where $G_{pq}^{(C,C)}$ is the third rail's conductance between bus p and q , $G_{pq}^{(C,R)}$ and $G_{pq}^{(R,C)}$ are the conductance between the third rail and running rail and in between bus p and q , $G_{pq}^{(R,R)}$ is the running rail's conductance between p and q .

2. Three-level conductor systems

A two-level conductor system per bus is a system that is used with a typical DGM and N-DGM. The conductance matrices $[G]$ are formed by the conductance submatrices for each bus as shown in (13)-(15) [21].

$$[G_s] = \begin{bmatrix} \frac{1}{R_s} & -\frac{1}{R_s} & 0 \\ -\frac{1}{R_s} & \frac{1}{R_s} + \frac{1}{R_{SE}} & 0 \\ 0 & -\frac{1}{R_{SE}} & \frac{1}{R_{SE}} \end{bmatrix} \quad (13)$$

$$[G_{pq}] = [G_{qp}] = \begin{bmatrix} \frac{1}{dR'_C} & 0 & 0 \\ 0 & \frac{1}{dR'_R} & 0 \\ 0 & 0 & \frac{1}{dR'_S} \end{bmatrix} \quad (14)$$

$$[G_{pp}]_{SE} = [G_{qq}]_{SE} = \begin{bmatrix} 0 & 0 & 0 \\ 0 & dG'_{RS} & -dG'_{RS} \\ 0 & -dG'_{RS} & dG'_{RS} + dG'_{SE} \end{bmatrix} \quad (15)$$

where $G_{pq}^{(C,C)}$ is the third rail's conductance between bus p and q , $G_{pq}^{(C,R)}$ and $G_{pq}^{(R,C)}$ are the conductance between the third rail and running rail and in between bus p and q , $G_{pq}^{(C,S)}$ and $G_{pq}^{(S,C)}$ are the conductance between the third

rail and structure and in between bus p and q , $G_{pq}^{(R,R)}$ is the running rail's conductance between p and q , $G_{pq}^{(R,S)}$ and $G_{pq}^{(S,R)}$ are the conductance between the running rail and structure and in between bus p and q , and $G_{pq}^{(S,S)}$ is the structure's conductance between p and q .

Therefore, the nodal equation for the whole Nbus system is obtained in (16) and (17) for two-level [17] and three-level conductor systems [21] respectively.

The current matrix $[I]$ in (9) would be formed by taking into account the substation current (I_s) and the train current (I_{tr}) in (18), where P_T and V_T are the required power and voltage of the train, according to the bus being considered. Ultimately, the bus voltages matrix $[V]$ can be obtained by solving in (9). This process has been conducted iteratively until the maximum approximate error of each bus voltage mismatch is less than the pre-defined value or the iteration time reaches the final time [17, 18, 21].

$$I_{tr} = \frac{P_T}{V_T} \quad (18)$$

$$\begin{bmatrix} I_1^{(C)} \\ I_1^{(R)} \\ I_2^{(C)} \\ I_2^{(R)} \\ \vdots \\ I_N^{(C)} \\ I_N^{(R)} \end{bmatrix} = \begin{bmatrix} \begin{bmatrix} G_{11}^{(C,C)} & G_{11}^{(C,R)} \\ G_{11}^{(R,C)} & G_{11}^{(R,R)} \end{bmatrix} & \begin{bmatrix} G_{12}^{(C,C)} & G_{12}^{(C,R)} \\ G_{12}^{(R,C)} & G_{12}^{(R,R)} \end{bmatrix} & \vdots & \begin{bmatrix} G_{1N}^{(C,C)} & G_{1N}^{(C,R)} \\ G_{1N}^{(R,C)} & G_{1N}^{(R,R)} \end{bmatrix} \\ \vdots & \vdots & \ddots & \vdots \\ \begin{bmatrix} G_{N1}^{(C,C)} & G_{N1}^{(C,R)} \\ G_{N1}^{(R,C)} & G_{N1}^{(R,R)} \end{bmatrix} & \begin{bmatrix} G_{N,N-1}^{(C,C)} & G_{N,N-1}^{(C,R)} \\ G_{N,N-1}^{(R,C)} & G_{N,N-1}^{(R,R)} \end{bmatrix} & \vdots & \begin{bmatrix} G_{NN}^{(C,C)} & G_{NN}^{(C,R)} \\ G_{NN}^{(R,C)} & G_{NN}^{(R,R)} \end{bmatrix} \end{bmatrix} \begin{bmatrix} V_1^{(C)} \\ V_1^{(R)} \\ V_2^{(C)} \\ V_2^{(R)} \\ \vdots \\ V_N^{(C)} \\ V_N^{(R)} \end{bmatrix} \quad (16)$$

$$\begin{bmatrix} I_1^{(C)} \\ I_1^{(R)} \\ I_1^{(S)} \\ I_2^{(C)} \\ I_2^{(R)} \\ I_2^{(S)} \\ \vdots \\ I_N^{(C)} \\ I_N^{(R)} \\ I_N^{(S)} \end{bmatrix} = \begin{bmatrix} \begin{bmatrix} G_{11}^{(C,C)} & G_{11}^{(C,R)} & G_{11}^{(C,S)} \\ G_{11}^{(R,C)} & G_{11}^{(R,R)} & G_{11}^{(R,S)} \\ G_{11}^{(S,C)} & G_{11}^{(S,R)} & G_{11}^{(S,S)} \end{bmatrix} & \begin{bmatrix} G_{12}^{(C,C)} & G_{12}^{(C,R)} & G_{12}^{(C,S)} \\ G_{12}^{(R,C)} & G_{12}^{(R,R)} & G_{12}^{(R,S)} \\ G_{12}^{(S,C)} & G_{12}^{(S,R)} & G_{12}^{(S,S)} \end{bmatrix} & \vdots & \begin{bmatrix} G_{1N}^{(C,C)} & G_{1N}^{(C,R)} & G_{1N}^{(C,S)} \\ G_{1N}^{(R,C)} & G_{1N}^{(R,R)} & G_{1N}^{(R,S)} \\ G_{1N}^{(S,C)} & G_{1N}^{(S,R)} & G_{1N}^{(S,S)} \end{bmatrix} \\ \vdots & \vdots & \ddots & \vdots \\ \begin{bmatrix} G_{N1}^{(C,C)} & G_{N1}^{(C,R)} & G_{N1}^{(C,S)} \\ G_{N1}^{(R,C)} & G_{N1}^{(R,R)} & G_{N1}^{(R,S)} \\ G_{N1}^{(S,C)} & G_{N1}^{(S,R)} & G_{N1}^{(S,S)} \end{bmatrix} & \begin{bmatrix} G_{N,N-1}^{(C,C)} & G_{N,N-1}^{(C,R)} & G_{N,N-1}^{(C,S)} \\ G_{N,N-1}^{(R,C)} & G_{N,N-1}^{(R,R)} & G_{N,N-1}^{(R,S)} \\ G_{N,N-1}^{(S,C)} & G_{N,N-1}^{(S,R)} & G_{N,N-1}^{(S,S)} \end{bmatrix} & \vdots & \begin{bmatrix} G_{NN}^{(C,C)} & G_{NN}^{(C,R)} & G_{NN}^{(C,S)} \\ G_{NN}^{(R,C)} & G_{NN}^{(R,R)} & G_{NN}^{(R,S)} \\ G_{NN}^{(S,C)} & G_{NN}^{(S,R)} & G_{NN}^{(S,S)} \end{bmatrix} \end{bmatrix} \begin{bmatrix} V_1^{(C)} \\ V_1^{(R)} \\ V_1^{(S)} \\ V_2^{(C)} \\ V_2^{(R)} \\ V_2^{(S)} \\ \vdots \\ V_N^{(C)} \\ V_N^{(R)} \\ V_N^{(S)} \end{bmatrix} \quad (17)$$

Simulation scheme

As shown in the flowchart in Fig. 12, the simulation is initialised with setting up the relevant parameters and the variables needed in the process. Then, it goes to the main loop starting with the train movement calculation to

determine the motion characteristic of the train such as the speed, position, and the consumed power. If the train arrives at the last station, it terminates the calculation. Next, the network capture is performed to configure the power network: bus number arrangement, bus data, and line data. After that, the power flow calculation is carried

out to find the bus voltages, power and energy consumption at each substation, and power losses. Increment the time step and return to the main loop, iterates the calculation until the iteration time reaches the pre-defined final time [17, 21].

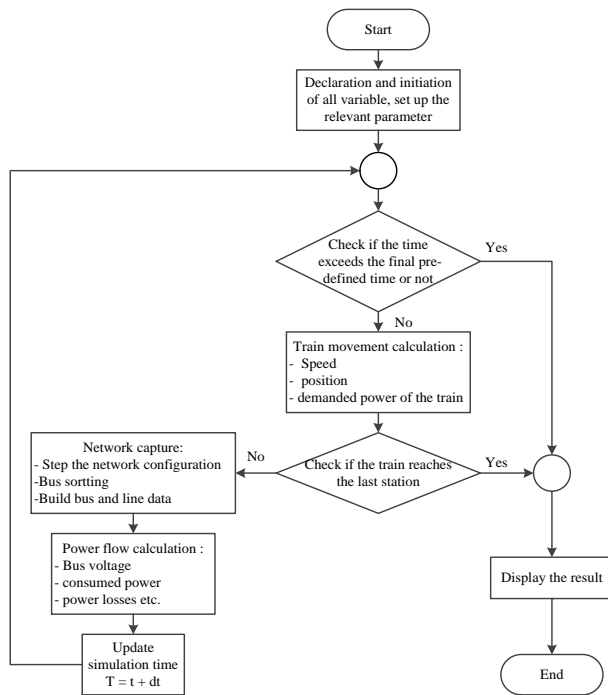


Fig. 12 The flowchart of the programmed sequence.

5. SIMULATION AND RESULTS

The MRT Chalong Ratchadham Line (MRT Purple line) of Bangkok's Metropolitan Rapid Transit system in Table 2 provides the service in Bangkok, Thailand and is the case study for the single-train movement simulation. It consists of 16 passenger stations and 10 rectifier substations. The passenger station's and traction substation's position, train and system data of the MRT Purple line are applied in this study. The nominal voltage of the train operation is 750 VDC, 2x2.5 MW supplied from the traction substations via the third rail. The line route and stations are illustrated in APPENDIX.

The single-train movement simulation program has been implemented in MATLAB/M-file using the proposed model, train movement calculation, and power flow calculation described above. The program simulates the MRT Purple line, running between stations Khlong Bang Phai and Tao Poon with 25 seconds dwell time for stopping at every station.

Simulation results

The train speed is controlled by a proportional control for NGM system, shown in Fig. 14. The results are expected to obtain rail potential, power and voltages at each TSS, the train's consumed power, energy demand at substations and the voltage profile of the train see Fig.15-21.

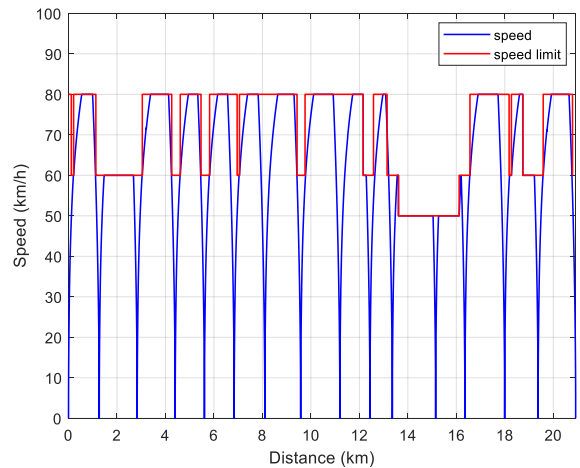


Fig. 14. The train's speed profile.

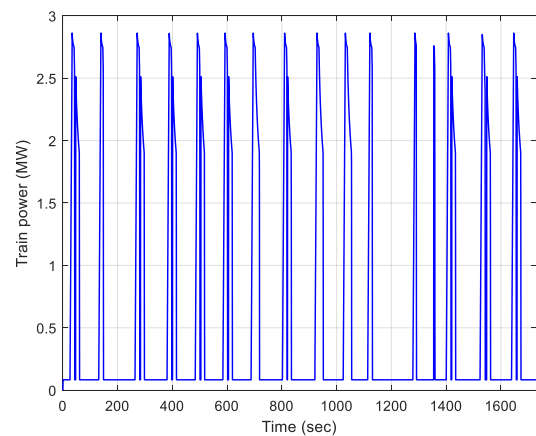


Fig. 15. The power consumed by the train.

Fig. 14 shows the train speed along the distance it moves through with the red line served as the arbitrarily specified speed command.

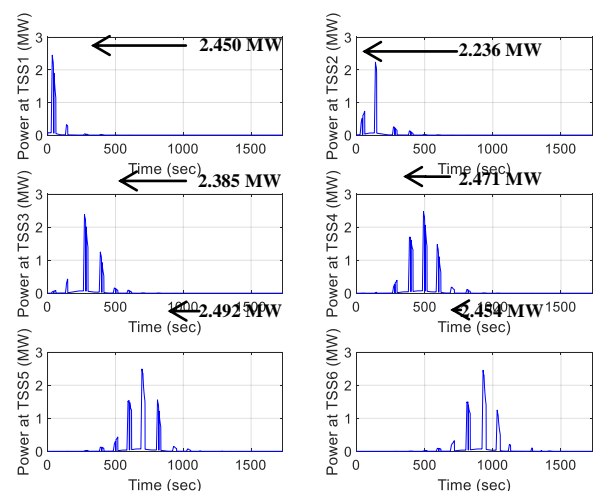


Fig. 16. The power at TSS 1-6.

The train draws power during acceleration and speed control mode for attractive purpose and consumes only the auxiliary power during stopping at the station as shown in Fig. 15. Figure 16-17 shows the power and voltage at traction substation 1-6 and at the train's

position when the train runs near the traction substation. The power traction substation will provide power over the distant traction substation. In the same way, the voltage at the TSS close to the train may tend to drop below the normal voltage.

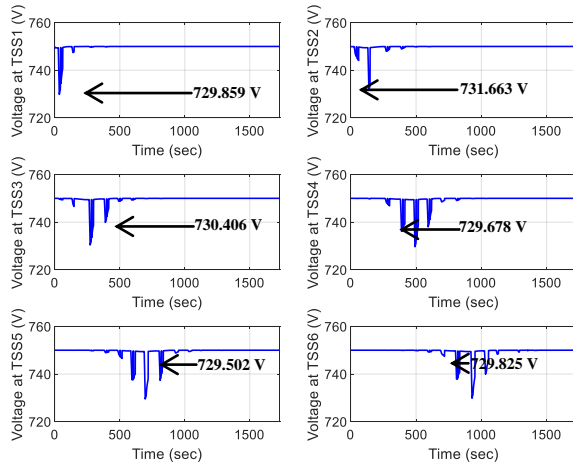


Fig. 17. The voltage at TSS 1-6.

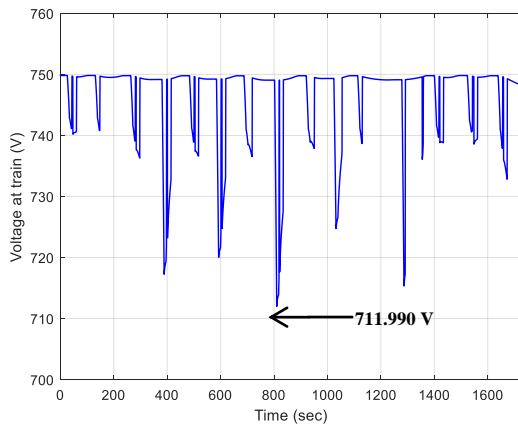


Fig. 18. The train's voltage.

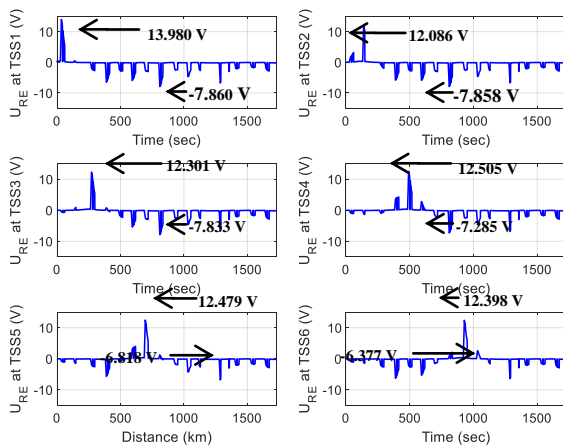


Fig. 19. Rail potential at TSS 1 – 6.

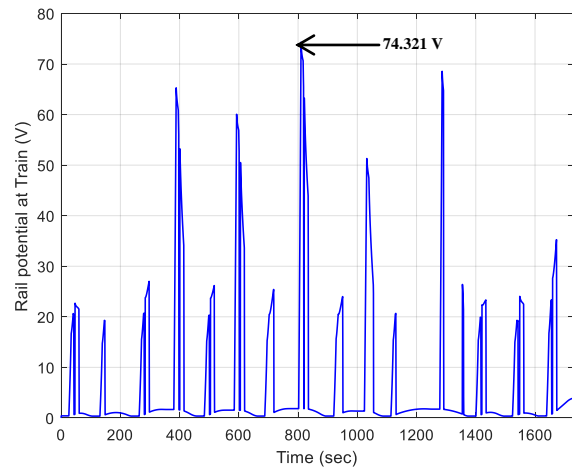


Fig. 20. Rail potential at the train's position.

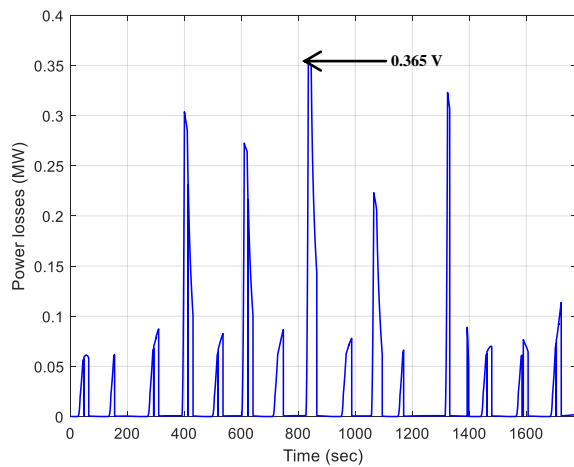


Fig. 21. Power losses.

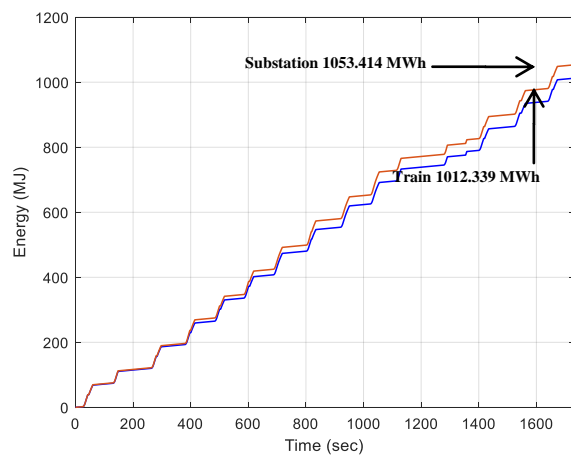


Fig. 22. The cumulative energy of the train and all TSSs.

The Rail potential of the rail-to-earth at the traction substation 1-6 and at the train's position shown in Fig. 19-20, the maximum rail potential is 13.98 V at TSS and 74.31 V at the train's position respectively see in Table 1. This may be due to a large amount of current flowing to the train at that time due to the acceleration and the spacing of the propulsion station. According to European standards, the maximum trajectory that occurs is less than the maximum permissible accessible voltage in less

than 300 seconds and the voltage does not exceed 120 Vdc [5]. Therefore, for this case, it is assumed that the standard is passed.

The power losses and cumulative electrical energy of the train and all TSSs are shown in Fig. 21 and 22, respectively, depicting that the energy fed from TSS appeared to be greater than the energy drawn by the train which implies that there must be energy lost in the transmission, due to train efficiency, etc. In the end, the total energy loss was found to be 82.33 MWh as seen in the gap between the train's and TSS's curve in Fig. 21.

Simulation results comparison

The comparison of simulation results with NGM, DGM and N-DGM showed that the electrical values (max. power, min. voltage, max. and min. rail potential, max. and min. rail to structure voltage, max. and structure to earth voltage at TSS, and maximum power, min. voltage, max. potential and max. structure to earth voltage, and some power all TSS, sum power at train and sum power losses) were similar see Table 1. The DGM and N-DGM methods, the DGM and N-DGM models have similar energy demand and are less than 0.087% NGM model. Therefore, the NGM model is suitable for general consideration and when needed for the DGM model can be used instead of the N-DGM model.

In addition, the structure voltage at the traction substation 1-6 shown in Fig 23. shows that the maximum voltage in the topology is 0.712 V at TSS for DGM. The structure voltage at the train's position shown in Fig. 24. shows that the maximum voltage in the topology are and 0.766 V at the train's position.

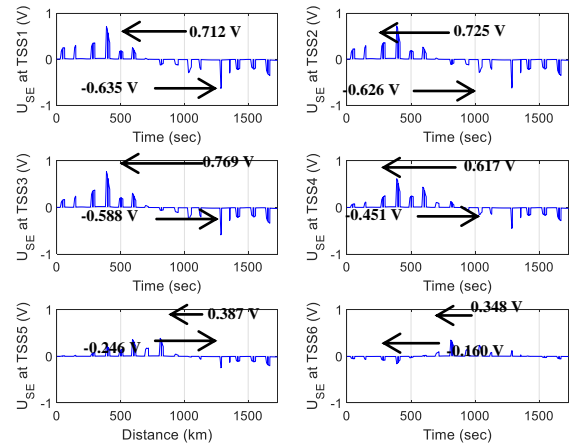


Fig. 23 Rail potential at TSS 1 – 6.

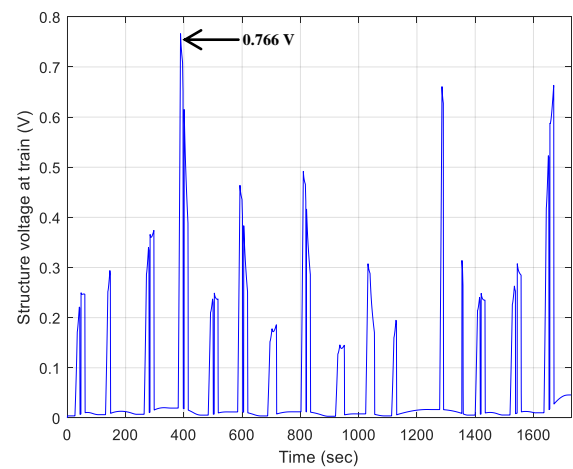


Fig. 24 Rail potential at the train's position.

Table 1. Comparison of the Simulation Results of the Earthing System

Parameter		NGM	DGM	N-DGM
TSS	Maximum power (MW)	2.542	2.541	2.541
	Minimum voltage (V)	729.080	729.085	729.085
	Maximum rail potential (V)	13.981	13.980	13.980
	Minimum rail potential (V)	-7.889	-7.860	-7.860
	Maximum rail to structure voltage (V)	-	13.808	13.808
	Minimum rail to structure voltage (V)	-	-7.735	-7.735
	Maximum structure to earth voltage (V)	-	0.712	0.769
	Minimum structure to earth voltage (V)	-	-5.54	-0.650
Train	Maximum power (MW)	2.861	2.861	2.861
	Minimum voltage (V)	711.990	712.015	712.015
	Maximum rail potential (V)	74.312	74.354	74.354
	Maximum structure to earth voltage (V)	-	0.766	0.766
Sum energy at TSS (MWh)		1053.414	1052.493	1052.493
Sum energy at train (MWh)		1012.339	1011.410	1011.410
Sum energy losses(MWh)		82.233	82.249	82.249

Based on the simulation results in the case of NGM, DGM and N-DGM, electrical parameters have similar values, so it depends on the use of the model. NGM models are suitable for general considerations, and when considering the voltage in the structure at the substation and train, the DGM and N-DGM models should be used. In addition to simplifying the simulation, the DGM model should also be used instead of the N-DGM model, but if looking at a more detailed elevation structure, the N-DGM model should be applied.

6. CONCLUSION

The proposed single-train movement model was developed and successfully implemented in the simulation. According to the results, it could evaluate the rail potential, structure voltage, energy demand at a substation and the voltage profile of the train during the train movement. Moreover, it is capable of the simulation of studying the performance of the railway systems with thorough consideration of rail potential based on the permissible European standard and the structure voltage. For further study, this paper could apply to study the stray current in the structure of the DC railway systems.

In addition, by comparing the earthing model by NGM, DGM and N-DGM methods, the DGM and N-DGM models have similar energy demand and are less than 0.087% NGM model. Therefore, the NGM model is suitable for general consideration and when needed for the DGM model can be used instead of the N-DGM model.

ACKNOWLEDGMENT

We would like to express our sincere gratitude to the Thailand Research Fund through the Research and Researchers for Industries-RRI Ph.D. Program for supporting this research.

REFERENCES

- [1] Friedrich, K. Rainer P. Axel, S. and Egid, S. 2009. *Contact Lines for Electric Railways: Planning, Design, Implementation, Maintenance*. 2nd edn. Publicis Publishing.
- [2] Chien, H. L. 2005. Evaluation of the Maximum Potential Rise in Taipei Rail Transit Systems. *IEEE Transactions on power delivery* 20(2): 1379-1384.
- [3] Chien, H. L. and Chien, J. L. 2006. Assessment of Grounding Schemes on Rail Potential and Stray Currents in a DC Transit System. *IEEE Transactions on power delivery*, 21(4): 1941-1947.
- [4] Liu, Y. C. and Chen, J. F. 2005. Control scheme for reducing rail potential and stray current in MRT systems. *IEE Proc.-Electr. Power Apply*. 152(3): 612-618.
- [5] British Standards Institution. BS EN 50122-1. 2011. Railway applications - Fixed installations - Electrical safety, earthing and the return circuit - Part 1: Protective provisions against electric shock, London: BSI.
- [6] British Standards Institution. BS EN 50122-2. 2010. Railway applications - Fixed installations - Electrical safety, earthing and the return circuit - Part 2: Provisions against the effects of stray currents caused by d.c. traction systems, London: BSI.
- [7] Niasati, M. and Gholami, A. 2005. Evaluation of Rail Potential Control Devices Performance for Control of Rail Potential of DC Electrified Railway Systems. *Railway Engineering-Challenges for Railway Transportation in Information Age*: 1-7.
- [8] Yu, J. G. and Goodman, C. J. 2005. Modelling of Rail Potential Rise and Leakage Current in DC Rail Transit Systems. *Stray Current Effects of DC Railways and Tramways, IEE Colloquium* 2(2): 1 - 6.
- [9] Chen, S. L. Hsu, S. C. Tseng, C. T. Yan, K. H. Chou, H. Y., and Too, T.M., 2006. Analysis of Rail Potential and Stray current for Taipei Metro. *IEEE Transactions on vehicular technology* 55(1): 67-75.
- [10] Tzeng, Y. S. and Lee, C. H. 2010. Analysis of Rail Potential and Stray currents in a Direct-Current Transit System. *IEEE Transactions on power delivery* 25(3): 1516-1525.
- [11] Valero, R. J. Sanz, F. J. Calculation of remote effects of stray currents on rail voltages in dc railways systems, *IET Electrical Systems in Transportation*, 2013, 3(2), pp. 31-40.
- [12] Yu-qiao, W. Wei, L. Xue-feng, Y. Guo, Y. Qi-gao, F. and Li-ping, Z. Modeling and simulation the distribution of metro stray current, *2010 International Conference on Computer Application and System Modeling (ICCSM 2010)*, China, 22-24 October 2010, pp. 704-707.
- [13] Fichera, F. Mariscotti, A. Ogunsola, A. Sandrolini, L. Comparison of distributed and lumped parameters stray current models, *IEEE African Conference (AFRICON 2013)*, Mauritius, 9-12 September 2013, pp. 1-5.
- [14] Fichera, F. Mariscotti, A. Ogunsola, A. Evaluating stray current from DC electrified transit systems with lumped parameter and multi-layer soil models, *International Conference on Computer as a Tool (EUROCON 2013)*, Croatia, 1-4 July 2013, pp. 1187-1192.
- [15] Charalambous, C. A. Cotton, I. Aylott, P. A Simulation Tool to Predict the Impact of Soil Topologies on Coupling Between a Light Rail System and Buried Third-Party Infrastructure, *Vehicular Technology, IEEE Transactions*, 2008, 57(3), pp. 1404-1416.
- [16] Jorge, V. R. and Javier, S. F. Calculation of remote effects of stray currents on rail voltages in dc railways systems, *IET Electrical Systems in Transportation* 2013, 3(2), pp. 31-40.
- [17] Mongkoldee, K. Leeton, U. and Kulworawanichpong, T. 2016. Single train movement modeling and simulation with rail potential consideration. *Proceedings of the 2016 IEEE/SICE International Symposium on System Integration*. Sapporo, Japan, December 13-15, 2016.

- [18] Kulworawanichpong, T. 2015. Multi-train modeling and simulation integrated with traction power supply solver using simplified Newton-Raphson method. *Journal of Modern Transportation*: 1-11.
- [19] Japanese national Industrial Standard. JIS E 6002. 1989. General Rules for Performance of Electric Railcars for Commuter Use. Japan.
- [20] Stell R. W. B. 2011. Maximum permissible rail potential, DC Traction Power Systems. *Vehicular Technology Magazine, IEEE*, 6(3): 99-105.
- [21] Chuchit, T. Ratniyomchai, T. Kulworawanichpong, T. 2018. Simulation of Stray Current in DC Railways System with Rail Potential and Structure Voltage. *International Journal of Industrial Electronics and Electrical Engineering (IJIEEE)*. 6(6): 32-38.
- [22] Sumpavakup, C. Ratniyomchai, T. Kulworawanichpong, T. 2017. Optimal energy saving in DC railway system with on-board energy storage system by using peak demand cutting strategy. *Journal of Modern Transportation* 25(4): 223-235.

APPENDIX

The line route and stations of MRT Purple line, Bangkok, Thailand shown in Table 2. And parameter for simulation showed in Table 3.

Table 2. MRT Purple line data, Bangkok, Thailand

Station code	Station Name	Distance	Route map
PP01	Khlong Bang Phai	0.00	
PP02	Talad Bang Yai	1.27	
PP03	Sam Yaek Bang Yai	1.56	
PP04	Bang Phlu	1.57	
PP05	Bang Rak Yai	1.20	
PP06	Bang Rak Noi - Tha It	1.25	
PP07	Sai Ma	1.25	
PP08	Phra Nangklao Bridge	1.47	
PP09	Yaek Nonthaburi 1	1.63	
PP10	Bang Krasor	1.26	
PP11	Nonthaburi Civic	0.90	
PP12	Ministry of Public	1.79	
PP13	Yaek Tiwanon	1.20	
PP14	Wong Sawang	1.72	
PP15	Bang Son	1.29	
PP16	Tao Poon	1.58	

Table 3. Specific data of MRT Purple line, Bangkok, Thailand

Specific data	Information	
Train parameters		
Weight	tare weight	153 ton
	payload AW3	75 ton
Movement Feature	max. speed	80 km/h
	max. acceleration	1.2 m/s ²
	max. deceleration	0.9 m/s ²
Efficiency	gear	98%
	motor	90%
	motor power factor	86%
	inverter	96.5%
Auxiliary power	constant load	270 kW
Train resistance	equation (5)	
TE curve	max. TE	228.8 N
	v_1	30 km/h
	v_2	55 km/h
Route	Khlong Bang Phai station -> Tao Poon station	
Station dwell time	25 sec	
3 rd Rail Resistance	0.007 ohms/km at 15 degree C (+10% Temperature)	
Running Rail Resistance (in parallel)	0.0175 ohms/km at 20 degree C (+10% Temperature)	
rail-to-structure conductance per unit length	0.1 S/km	
structure's resistor	0.1 ohms/km	
structure-to-earth conductance per unit length	0.1 S/km	
Distance of d	10 m (0.01 km)	
distance of pier	40 m (0.04 km)	